Polymer Bulletin 31, 235–241 (1993)

Polymer Bulletin

Fracture mechanical characterization and damage zone development in glass fiber mat-reinforced thermoplastics*

J. Karger-Kocsis

Institut für Verbundwerkstoffe GmbH, Universität Kaiserslautern, Postfach 3049, D-67663 Kaiserslautern, Germany

ABSTRACT

It was established that reliable fracture mechanical values of glass mat-reinforced thermoplastics (GMT) can be determined only by using specimens of proper dimensions. The free ligament width of the specimens (W-a, where W is the specimen width and a is the notch length) should exceed ca. 15 mm due to the large damage zone developed. The size of the damage zone was determined on modified compact tension (CT) specimens by localizing the acoustic emission (AE) events during loading. The damage zone was strongly underestimated when light microscopic (LM) pictures, taken during the loading of the specimens, were considered. Simultaneous monitoring of the failure by AE and LM allowed to assign the failure events and to assess the failure sequence, as well. It was supposed that the size of the damage zone and thus the load transfer within, strongly depend whether the stress-strain characteristics of the matrix and that of the reinforcing mat are matched or not.

1. INTRODUCTION

Althouh glass mat-reinforced thermoplastics (GMT) with different matrices, such as polypropylene (PP) and nylon block copolymer (NBC), are widely used in different applications, limited information is available on their fracture and failure behavior [1-5]. Even less works were performed on the fracture mechanical characterization of GMT [4-5]. Fracture mechanical data reflecting the inherent material properties are linked to secimens of given dimensions. These size criteria are settled for unfilled polymers and, in addition, they seem to work also for filled and chopped fiber-reinforced composites. First studies on the fracture mechanical response of GMTs [4-6] indicate a strong effect of the free ligament width (W-a, where W is the width of the specimen and "a" is the notch lenght). Aims of the present paper are: i) to study the effects of specimen size on fracture mechanics values, ii) to estimate the damage zone size, and iii) to clarify the failure mode in GMT materials.

2. EXPERIMENTALS

2.1. Materials

The GMTs investigated were produced either by reaction injection molding (RIM; NBC-SRIM composites) or by pressing a needle-punched loose textile preform consisting of glass fiber swirl mat (GF-mat) and non-woven polypropylene (PP) layers. The volume fraction (V_f) of the GF mat was set for ca. 20 and 30 vol.%, respectively. Further details about the materials and processing parameters can be taken from refs. [5-6].

*Work presented at the ICCM-9 Conference (12–16 July, 1993) in Madrid, Spain

2.2. Fracture Mechanical Testing

The dynamic fracture toughness (K_d) and initiation fracture energy ($G_{d,i}$; taking into account the energy absorption in the crack initiation stage, i.e. up to the maximum load, F_{max}) were determined from Charpy measurements conducted on notched specimens at room temperature (RT). Dimensions of the Charpy specimens used were the followings: overall length: 120 mm, span length: 70 mm, thickness (B): 1.5 to 4 mm, width (W) 10 and 20 mm, respectively. The a/W ratio, where a is the notch length, was set between 0.05 and 0.6. The Charpy specimens were subjected to instrumented impact bending using the AFS-MK4 fractoscope of Ceast (Torino, Italy). Detailed information about the experiments and data reduction methods can be taken from ref. [5].

2.3. Failure Characteristics

Transmitted light microscopic (LM) pictures were taken during the loading of an enlarged CT-specimen [3,7] with simultaneous monitoring and location of the acoustic emission (AE). AE was detected by a Defektophone NEZ 220 analyzer of the Central Research Institute of Physics (Budapest, Hungary) using wide bandwith transducers (20-1000 kHz) with built-in preamplifiers [3,7].

3. RESULTS

3.1. Fracture Mechanical Data

Figure 1 shows the evaluation of both K_d and $G_{d,i}$ on a GF mat-reinforced PP and evidences a large scatter in the experimental data. This high scatter is caused by the local arrangement of the GF-mat in the crack tip, which "smears" the effects of the specimen width, at least from the point of view of K_d determination. In Figure 1 those specimens are also included (shaded field) which failed away from the razor blade notch. From the lower threshold value of this field, the "inherent" flaw size (a_{eff}) can be derived. The apparance of this inherent flaw can be attributed to the notch-rising effect of machining of the specimens and to the local "structuring" of the GF mat reinforcement.
In Figure 1b the effect of specimen width (W) turns out very clearly. $G_{d,i}$ is strongly underestimated when Charpy specimens of W=10 mm are impacted. It should be noted here, that $G_{d,i}$ did not rise when specimens with W>20 mm were investigated. Values of a_{eff} determined by the method of Akay and Barkley [8] agree with those got from the $\sigma.Y$ vs $a^{-1/2}$ plot (cf. Figure 1a).

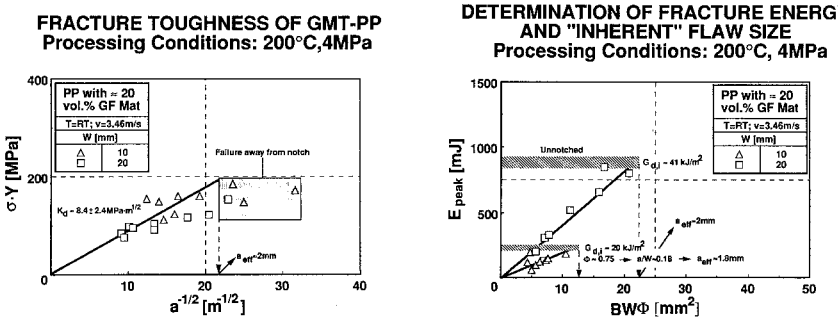

a) b)

Figure 1
Evaluation of K_d (a) and $G_{d,i}$ (b) by using notched Charpy specimens of different width (W) for GMT-PP with $V_f \approx 20$ vol.%.

The above results indicate for specimen size dependence of fracture mechanics values, especially when fracture energy is evaluated. Since this dependence of specimen size must be linked to the size of the damage zone emerged by loading, attention was focussed next on the assessment of the size of the damage zone. This task was extended by the study of the failure mode in order to elucidate the effect of V_f on the fracture toughness (K_d) and initiation fracture energy ($G_{d,i}$). Both of them decreased with increasing fiber mat content [4,6]. This indicates that balanced stiffness and toughness characteristics of GMTs are relied with an optimum reinforcement content (later it will be shown that the relation between stiffness and toughness is affected also by mat characteristics).

3.2. Damage Zone Size

Bright field LM pictures taken during the loading of a CT-specimen together with the related force-load line displacement (F-v_{LL}) curve are depicted in Figure 2a and b, respectively for the GMT-PP with $V_f \approx 20$ vol.% GF mat. Based on Figure 2a one could conlude for the damage zone at F_{max} a circular shaped one with about 5 mm diameter (becoming opaque by stress-whitening). The F-v_{LL} curve in Figure 2b was "sectioned" (I,II and III) in order to analyze the AE signals and to conclude the failure mode, as well [3,7].

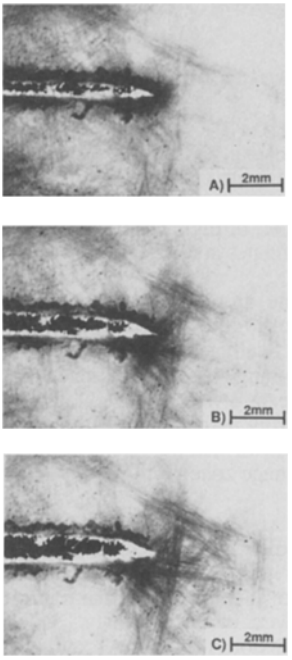

a)

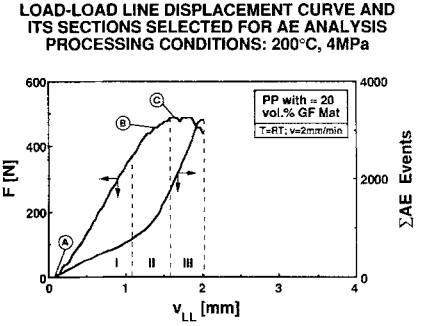

b)

Figure 2
a) Serial photographs taken during the loading of a CT-specimen cut from the GMT-PP with $V_f \approx 20$ vol.%

b) Corresponding F-v_{LL} curve and the cumulative run of the AE events
Note: this figure indicates both the taking position of the photographs in Figure 2a and the sectioning of the F-v_{LL} curve for AE signal analysis

Figure 3 displays the relative frequency of the amplitude distribution of the located AE events in range I+II of Figure 2b after scanning the surface of the specimen with circles of 6 mm diameter. Both the position and size of the damage zone becomes more clearly perceptible by this mathematical "weighing" procedure. Figure 3 clearly shows that the

damage zone determined by localization of the AE events is much larger than approached by LM. The size of the damage zone in this case could be estimated by a circle of 26 mm diameter. The criterion applied for the damage zone assessment was: which is that ellipse of minimum surface in which more than 75% of all located AE events can be found?

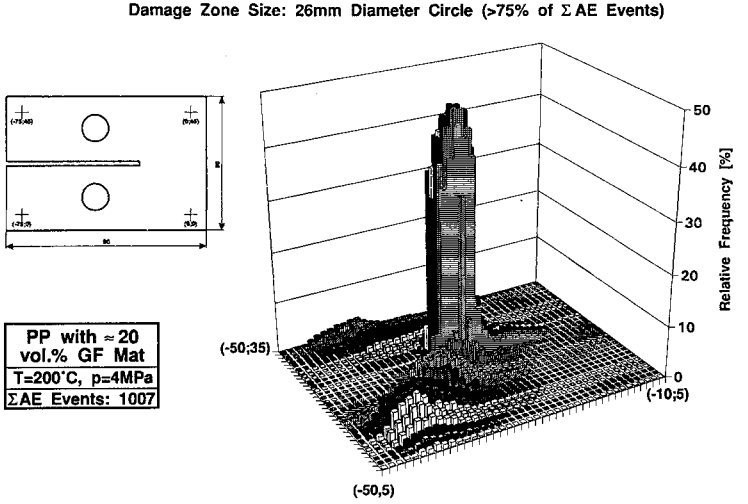

Figure 3
Weighed relative frequency of the located AE events in a GMT-PP with $V_f \approx 20$ vol.% produced by scanning the AE events with circles of 6 mm diameter
Notes: these figures are related with the ranges I+II of Figure 2b; the position of the AE transducers with the corresponding coordinates are indicated as well

Figure 4 shows the development of the damage zone along with the differential distribution of the amplitude in the sections I,II and III of Figure 2b. Based on Figure 4 one can conclude that the size of the damage zone is practically constant up to F_{max}, i.e. until the onset of crack propagation. In the postmaximum range the damage zone tends to become smaller. It is obvious, since the growing crack means a well localized failure site. It should be underlined here, that not the full damage zone is penetrated into the free ligament (W-a), part of the damage zone can be resolved always at the flanks of the saw-cut notch. Increasing V_f did not result in an enhanced damage zone size [6].

3.3. Failure Sequence

Considering the AE signal characteristics, the amplitude distribution becomes wider with increasing loading and at the same time peaks at higher amplitudes emerge. Regarding the microscopically observed failure (cf. Figure 2a) and the results got on GF mat reinforced NBC, where the breakdown process could be followed unambiguously [3,7], the following failure modes can be predicted in the selected sections of the F-v_{LL} curve:

I- matrix deformation in the crack tip blunting process (damage zone development; amplitude <30 dB) which induces short and long-range debonding and partial splitting-up of the strand (peak amplitudes ≈50 and 60 dB, respectively).
II- strands laying parallel and in plane of the crack growth debond in a long distance (amplitude: 50-60 dB). Kinked strands sustaining bending stresses debond as well (amplitude 60-70 dB) and "filamentize" by fracture of the constituting filaments (splitting-up by fiber fracture at an amplitude of 80-85 dB).
III- in the postmaximum range to the above mentioned and parallel running failure events, breakage of the strands and their constituents (especially those under

bending stresses in course of the crack tip opening) associate. This can be attributed to fact that the mesh-type deformability of the GF strand mat has been exhausted (cf. later).

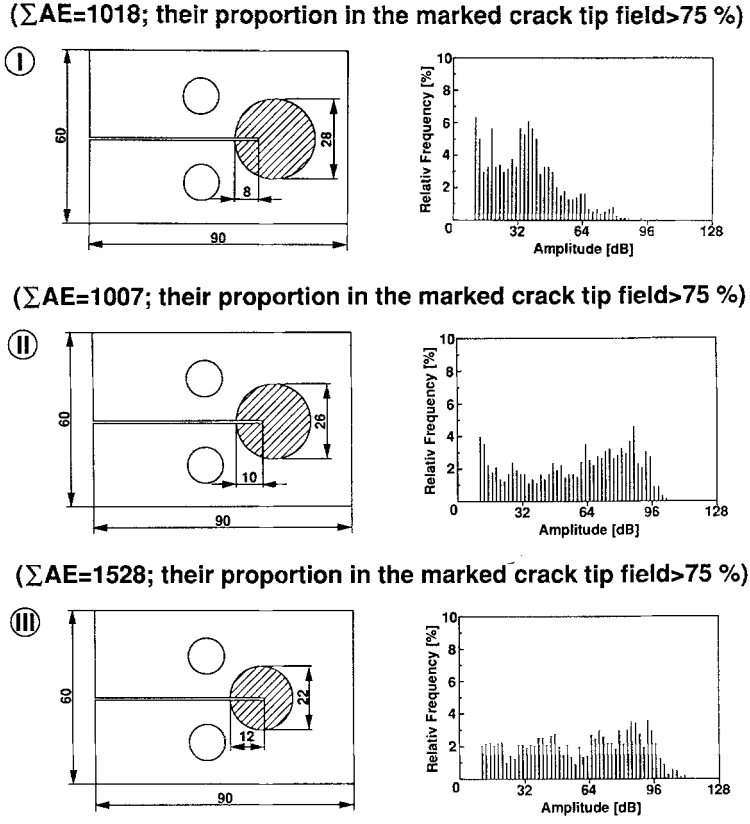

Figure 4
Development of the damage zone, as well as relative distribution of the located AE signal amplitudes in the range I (a), II (b) and III (c) of the F-v_{LL} curve in Figure 2b.
Note: the damage zone was determined by a home-made program by scanning the located AE events by ellipses as indicated in Figure 5.

The number of the AE events registered during the loading of the GMT-PP with $V_f \approx 30$ vol.% was less than registered at $V_f \approx 20$ vol%, at least up to Fmax. In addition, AE events of higher amplitudes were not monitored in this higly reinforced GMT-PP. This indicates that up to F_{max} debonding processes dominate in GMT-PP with high V_f. The AE events of high amplitude and energy were assigned to strand fracture, filamentization and pull-out processes. Their onset and run are impeded in a more stiff GMT with high V_f, that is the reason why they are lacking. Due to this "inherent" material stiffness, the mesh-type deformation of the mat and thus the further breakdown processes of high energy absorption are depressed. Provided that the above scenario still holds at dynamic conditions, the observed deterioration in K_d and $G_{d,i}$ (Figure 6) can be easily explained.

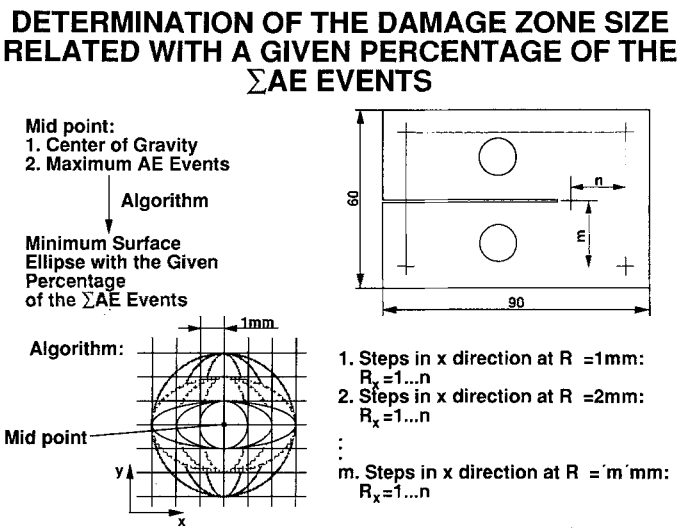

Figure 5
Route of determination of the size and shape of the damage zone, schematically

Comparing the with dependence of specimens, the failure sequence, the size and form of the damage zone established for both GF mat-reinforced PP [6] and NBC [3,7] composites, the similarities become obvious. The GF mat used in both matrices exhibited similar characteristics so that their in-plane deformability should be also analogous. This deformability, on the other hand, should depend on the mean "mesh size" of the mat, being responsible for the stress transfer and stress redistribution in the crack tip (at least in composites with matrices of low stiffness). The mat deformability, controlled by the mean mesh size, is affected by both matrix characteristics and testing parameters. The former effect was mentioned above, while the latter can be evidenced by considering the frequency embrittlement of the matrix at high strain rates (provided that crack tip heating does not compensate this effect). This suggests that the in-plane deformability of the composites and thus the related K_d and $G_{d,i}$ values depend how closely is matched the matrix deformability to that of the GF strand mat. With other words, the toughness performance of GMTs and GMT-like composites can be significantly improved by fitting the mat characteristics (network structure and its deformability) to those of the matrices. The main problem of this approach is related with the fact that the basic parameters of the reinforcing mats have not been studied so far in this respect. The surface weight of the mats and strength of their constituting filaments, which are mostly indicated in brochures of the manufacturers, do not give enough information for matching the stress-strain responses of the matrix and reinforcing mat both at out-of-plane and in-plane type loadings. It is needed therefore to characterize the reinforcing mats more adequately, probably by using methods of the mathematical statistics. Recent works published on determination of stiffness parameters of GMTs [9] support such an approach.

If both microstructure and mean mesh size of the reinforcing mat are analogous, then the run of the breakdown process should be also the same. That was the reason why the AE assignment evidenced for GF mat reinforced NBC [3,7] was applied also for GMT-PP (where the failure events based on LM can scarcely be resolved, if any; cf. Figure 2a). When the in-plane mesh type deformability of the mat is exhausted in a crack-opening type loading, the following failure steps become dominant: breaking-up of the strands laying under bending stress followed by intrastrand fracture and pull-out and strand pull-out processes. This failure sequence for GMTs has been proposed [4,7].

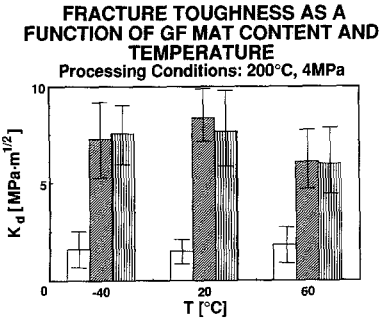

a)

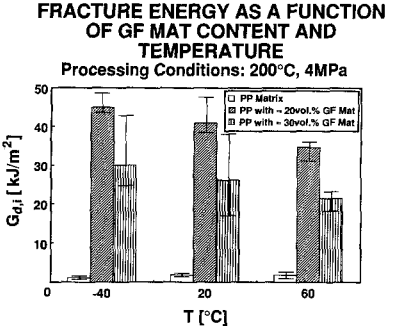

b)

Figure 6
Change in K_d (a) and $G_{d,i}$ (b) as a function of temperature and mat content

4. CONCLUSIONS

i) The size of the damage zone in glass mat-reinforced thermoplastics (GMT) can well be estimated by locating the acoustic emission (AE) events monitored during loading. It was shown that the extension of this zone can be adequately approached by a circle of about 30 mm diameter, the half of which penetrates into the free ligament of the specimen.

ii) Due to this very large damage zone, determination of fracture mechanical values requires the use of specimens of proper dimensions.

iii) Analogies between the course of AE events in function of the loading in different GMTs were attributed to an analogous mesh size which controls the deformability of the mat. This seems to determine the stress transfer in the crack tip and thus the shape and extension of the damage zone.

ACKNOWLEDGEMENT

The help in the experimental work by Mrs. Zs.Fejes-Kozma and Mr. G.Kozma (Technical University of Budapest, Hungary) is gratefully acknowleged.

REFERENCES

1 Berglund, L.A. and Ericson, M.L.,Glass Mat Reinforced Polypropylene, Chapter 3.5 in "Polypropylene: Structure, Blends and Composites" (Ed.:Karger-Kocsis, J.), Elsevier Appl. Sci., London 1993 (to appear)

2 Bigg, D.M., Manufacturing Methods for Long Fiber Reinforced Polypropylene Sheets and Laminates, Chapter 3.7 in "Polypropylene: Structure, Blends and Composites" (Ed.: Karger-Kocsis,J.), Elsevier Appl. Sci., London 1993 (to appear)

3 Karger-Kocsis, J., Yuan, Q. and Czigány, T., Polym.Bulletin, **28** (1992), pp.717-723

4 Karger-Kocsis, J., Microstructural Aspects of Fracture in Polypropylene and in its Filled, Chopped Fiber and Fiber Mat-Reinforced Composites, Chapter 3.4 in "Polypropylene: Structure, Blends and Composites" (Ed.:Karger-Kocsis, J.), Elsevier Appl.Sci., London 1993 (to appear)

5 Idem: J.Appl.Polym.Sci., **45** (1992), pp.1595-1609

6 Karger-Kocsis, J. and Fejes-Kozma, Zs., Mechanics of Composite Materials (Riga), **1993**, in press

7 Karger-Kocsis, J. and Czigány, T., J.Mater.Sci., **28** (1993), in press

8 Akay, M. and Barkley, D., Polym.Test., **7** (1987), pp. 391-404

9 Bushko,W.C. and Stokes,V.K., Polym.Eng.Sci., **13** (1992), pp. 309-316

Accepted May 21, 1993 C